

Nuclear translocation of the calcium-binding protein ALG-2 induced by the RNA-binding protein RBM22

P. Montaville ^{a,1}, Y. Dai ^{b,1}, C.Y. Cheung ^{c,1}, K. Giller ^a, S. Becker ^a, M. Michalak ^b, S.E. Webb ^c, A.L. Miller ^c, J. Krebs ^{a,d,*}

^a Department of NMR-based Structural Biology, Max Planck Institute for Biophysical Chemistry, Göttingen, Germany

^b Department of Biochemistry, University of Alberta, Edmonton, Canada

^c Department of Biology, The Hong Kong University of Science and Technology, Hong Kong, People's Republic of China

^d Institute of Biochemistry, Swiss Federal Institute of Technology (ETH), Zurich, Switzerland

Received 18 July 2006; received in revised form 31 August 2006; accepted 1 September 2006

Available online 14 September 2006

Abstract

By yeast two-hybrid screening using the calcium-binding protein ALG-2 as bait a new target of ALG-2 was identified, the RNA-binding protein RBM22. In order to confirm these interactions *in vivo* we prepared fluorescent constructs by using the monomeric red fluorescent protein to label ALG-2 and the enhanced green fluorescent protein to label RBM22. Confocal microscopy of NIH 3T3 cells transfected with either ALG-2 or RBM22 expression constructs encoding fluorescent fusion proteins alone revealed that the majority of ALG-2 was localized in the cytoplasm whereas RBM22 was located in the nucleus. When cells were co-transfected with expression vectors encoding both fusion proteins ALG-2 was found in the nucleus indicating that RBM22 which can shuttle between the cytoplasm and the nucleus may play a role in nuclear translocation of ALG-2. Using zebrafish as a model mRNA homologues of ALG-2 and RBM22 were microinjected into the blastodisc-yolk margin of zebrafish embryos at the 1-cell stage followed by monitoring the fusion proteins during development of the zebrafish. Hereby, we observed that ALG-2 alone evenly distributed within the cell, whereas in the presence of RBM22 the two proteins co-localized within the nucleus. More than 95% of the two proteins co-localized within the same area in the nucleus suggesting a functional interaction between the Ca²⁺-signaling protein ALG-2 and the RNA-binding protein RBM22.

© 2006 Elsevier B.V. All rights reserved.

Keywords: ALG-2, RBM22; Ca²⁺-binding protein; RNA-binding protein; Zebrafish development; Confocal microscopy

1. Introduction

The pivotal role of Ca²⁺ as a general regulator of cellular functions is made possible due to the tightly controlled steep concentration gradient of ionized Ca²⁺ across cellular membranes. If a cell becomes activated due to an external signal this often results in up to a 100-fold rise in the intracellular free Ca²⁺ concentration due to the uptake of extracellular Ca²⁺ and/or the release of Ca²⁺ from intracellular stores. These changes of the

free Ca²⁺ concentration can cause significant oscillations of Ca²⁺ in the cytosol as well as in the nucleus providing the possibility of signal transduction for a number of different cellular activities such as metabolism, protein phosphorylation and dephosphorylation, fertilization, cell proliferation, division, gene expression and apoptosis, to name a few (for a recent review see Ref. [1]). Many of these functions are accomplished through the interaction of Ca²⁺ with specific proteins resulting in modulations of protein–protein interactions due to conformational changes of the Ca²⁺-receptors.

During our studies on the role of the Ca²⁺-binding protein ALG-2 [2,3] we identified a new protein interacting with ALG-2 using a yeast two-hybrid screening. This protein was an RNA-binding protein of unknown function [3] named RBM22 according to the GenBank (Accession No. NP_060517 for

* Corresponding author. Department of NMR-based Structural Biology, Max Planck Institute for Biophysical Chemistry, Göttingen, Germany. Tel.: +49 551 2012200; fax: +49 551 2012202.

E-mail address: jkrebs@nmr.mpibpc.mpg.de (J. Krebs).

¹ These authors contributed equally to this work.

hRBM22). ALG-2 interacting proteins like AIP1 [4] or Alix [5] had been identified by others before. RBM22 contains a conserved RNA-binding domain, a zinc finger of the unusual type C-x8-C-x5-C-x3-H, and the C-terminus is unusually rich in the amino acids Gly and Pro, including sequences of tetraprolins. The protein is highly conserved among invertebrates and vertebrates. A homolog containing the RNA-binding domain has also been found in yeast, and named either *slt11* [6] or *ECM2* (YBR065c; [7]) which was identified as a splicing factor involved in the activation and the assembly of the spliceosome [6]. Fig. 1 shows the aligned sequences of RBM22 of human, mouse, zebrafish, *Drosophila*, and *C. elegans* [8,9].

The recently completed nucleotide sequence of the human genome [10,11] revealed the surprising result that the whole genome only contained about 30,000 different genes, a number well below the amount of different proteins identified in cells. On the other hand, the high degree of proteomic complexity is achieved due to the fact that a single gene can generate structurally and functionally distinct protein isoforms due to alternative splicing [12,13]. Thus, it has been found that 75% of human genes are thought to encode at least two or more alternatively spliced isoforms [14,15].

Constitutive and alternative splicing of pre-mRNAs are complex processes which must be accomplished with high precision which is reflected by the complex machinery involved in splicing, the spliceosome, an organelle composed of over 100 different proteins [16,17] with a size in the order of 20 MDa [18], i.e. 4–5 times the size of a ribosome [18]. However, the way how the splicing process is controlled and regulated is poorly understood. Thus, impaired splicing can lead to severe cell damage and many diseases, including cancer [19]. Several laboratories used genome wide screening to identify essential proteins involved in the regulation of alternative splicing [20], in cell cycle [21], in zebrafish development [22] and in heart development of *Drosophila* [23]. All these studies identified homologues of RBM22 as being essential genes.

Here we provide evidence for the cellular co-localization of ALG-2 and RBM22 in tissue cultures and in zebrafish during development by using fluorescent constructs of the two proteins and confocal microscopy. The results indicate that due to the presence of RBM22, a typical nuclear protein, the cytosolic protein ALG-2 becomes translocated to the nucleus. These findings suggest that the formation of complexes between ALG-2 and RBM22 may thus play an important role in Ca^{2+} -dependent signaling influencing alternative splicing and cell division during development.

2. Materials and methods

2.1. Yeast two-hybrid screening

The cDNA encoding the full length human ALG-2 was cloned into plasmid *plexA* and then used as bait to screen a human peripheral blood cDNA library. Yeast transformation using the yeast strain L40 and screening were performed

by DUAL Systems Biotech AG, Zurich. Putative positive clones were verified by co-transformation with the bait plasmid into yeast, and their nucleotide sequences were analyzed.

2.2. Plasmid construction

The expression vector containing cDNA encoding ALG2-RFP has been generated by insertion of ALG-2 cDNA, obtained by PCR-driven amplification, into the *NheI* and *AgeI* sites of pRFP-N1. This vector, encoding for a monomeric variant of red fluorescent protein, was a generous gift from Dr. R. Y. Tsien, San Diego, USA. The expression vector containing cDNA encoding RBM22-GFP was generated by insertion of human RBM22 cDNA, obtained by PCR, into the *NheI* and *BamHI* sites of pEGFP-N3 (Clontech).

2.3. Mammalian cell culture

NIH 3T3 cells were plated in 24-well plates onto 12 mm cover slips and cultured at 37 °C and 5% CO₂ in Dulbecco's modified Eagle's medium (DMEM), containing 4.5 g/L D-glucose and 110 mg/L pyruvate, supplemented with 10% fetal calf serum, 2 mM glutamine and streptomycin/penicillin. After 24 h the cells were transfected at 80–90% confluency using either Roti-Fect (Roth) or lipofectamine according to the manufacturer's instructions. Transfections were performed with the single construct (0.5 µg plasmid DNA) or as co-transfections of the ALG-2 and the RBM22 expression vectors encoding fusion proteins (each 0.5 µg plasmid DNA) as detailed in Results. For confocal microscopy the cells were fixed with 3.7% formaldehyde 24 to 48 h after transfection. Mounting on object slides was performed with MOWIOL (10% (w/v) polyvinyl alcohol 4–88 (Fluka), 25% (w/v) glycerol, 0.1 M Tris-HCl, pH 8.5). Images have been taken using the confocal laser-scanning microscope LSM 5 from Zeiss (Carl Zeiss Canada Ltd.).

2.4. Embryo collection

Zebrafish (*Danio rerio*), AB strain, were maintained on a 14 h light/10 h dark cycle to stimulate spawning [24] and their fertilized eggs were collected as described elsewhere [25]. Embryos were placed in a custom-designed holding/imaging chamber [25], in 30% Danieau's solution (17.4 mM NaCl, 0.21 mM KCl, 0.18 mM Ca(NO₃)₂, 0.12 mM MgSO₄·7H₂O, 1.5 mM HEPES, pH 7.2) and maintained at ~ 28.5 °C throughout development.

2.5. Preparation of pSP64TNE-zRBM22-EGFP, pSP64TNE-zALG2-mRFP plasmids, and the control plasmids pSP64TNE-EGFP and pSP64TNE-mRFP

For the pSP64TNE-zRBM22-EGFP and pSP64TNE-zALG2-mRFP plasmids, the zRBM22-EGFP and zALG2-mRFP fragments were amplified from the pzRBM22-EGFP-N3 and pzALG2-mRFP-N1 plasmids, respectively using the following oligonucleotide primers: (1) For the pSP64TNE-zRBM22-EGFP plasmid, 5'-ACCAGCGCCGCATGGCGACGTCTTT-3' and 5'-ACCAGAA-TTCTTACTGTACAGCTC-3', and (2) for the pSP64TNE-zALG2-mRFP-N1 plasmid, 5'-ACCAGCGCCGCATGGCATATCATAA-3' and 5'-ACCAG-AATTCTTAGCGCCGGTGGAGTGGC-3'. The fragments were then cloned into the pSP64TNE plasmid [26] using *NotI* and *EcoRI*.

For the control plasmids, pSP64TNE-EGFP and pSP64TNE-mRFP, the EGFP and mRFP fragments were amplified from the pzRBM22-EGFP-N3 and pzALG2-mRFP-N1 plasmids, respectively using the following oligonucleotide primers: (1) For the pSP64TNE-EGFP, 5'-ACCAGCGCCGCATGGCCTCTCCGAGGAC-3' and 5'-ACCAGAATTCTTAGCGCCGG-TGGAGTGGC-3', and (2) for the pSP64TNE-mRFP, 5'-ACCAGCGCCGCATGGTGGCAAGG-3' and 5'-ACCAGAATTCTTACTTGTACAGCTC-3', and then cloned into the pSP64TNE plasmid using *NotI* and *EcoRI*.

Fig. 1. Alignment of the amino acid sequences of RBM22 from various organisms. Accession numbers of RBM22 sequences: (1) human NP_060517; (2) mouse AAH80205; (3) *Danio rerio* NP_998379; (4) *Drosophila melanogaster* NP_649440.3; (5) *C. elegans* NP_502014.2. The RNA-binding domain corresponds to amino acids 225–300 (human or mouse). The cysteins and the histidine of the conserved zinc finger Cx8Cx5Cx3H are indicated by an asterisk.

human (1) MATSLG - SNTYNRQNWEDADFPILCQTCCLGENPYIRMTKEKYGKECKICARPFTVFRWCPGVRMRFKKTEVCQTSKLNKVCQTCL
 mouse (1) MATSLG - SNTYNRQNWEDADFPILCQTCCLGENPYIRMTKEKYGKECKICARPFTVFRWCPGVRMRFKKTEVCQTSKLNKVCQTCL
 zebrafish (1) MATSLG - SNTYNRQNWEDSDFPILCQTCCLGENPYIRMTKEKFGKECKICARPFTVFRWCPGVRMRFKKTEVCQTSKLNKVCQTCL
 drosophila (1) SMSKST - TNTYNRQNWEDAEFPILCQTCCLGDNPYVRMIKERFGECKICTRPFITFRWCPGARMRFKKTEICQTCARLNKVCQTCL
 C. Elegans (1) SMSKSSYSQYNRKNWEDSDFPILCETCLGNNPYMRMMDKYGRCECKICERPFTFRWQPGKARYKNTLTCQTCARLNKVCQTCL
 Consensus (1) MATSLG SNTYNRQNWEDADFPILCQTCCLGENPYIRMTKEKYGKECKICARPFTVFRWCPGVRMRFKKTEVCQTSKLNKVCQTCL

human (86) LDLEYGLPIQVRDAGLSFKDDMPKSDVNKEYYTQNMEREISNSDGTTRPVGMIGK--ATSTSDMLLKLARTTPYYKRNRRPHICSFVW
 mouse (86) LDLEYGLPIQVRDAGLSFKDDMPKSDVNKEYYTQNMEREISNSDGTTRPVGMIGK--ATSTSDMLLKLARTTPYYKRNRRPHICSFVW
 zebrafish (86) LDLEYGLPIQVRDTGLSVKDEVRSDVNKEYYTQNMEREIANSDGTTRPVGLLGK--APSSDMLLKLARTTPYYKRNRRPHICSFVW
 drosophila (86) LDLEYGLPIQVRDAALKVADNMPQSDVNKEYYIQNIDAQLQDGDGTEAAGAVGR--SLAANEMLSKLARTAPYYKRNRRPHICSFVW
 C. Elegans (87) FDLEYGLPIQVRDHELQIADNIPKQGANRDFLQNVERTLGGDGTQPIAQIANMDQAAHRLRRMGRTQPYKRNRRPHICSFVW
 Consensus (87) LDLEYGLPIQVRDAGLSVKDDMPKSDVNKEYYTQNMEREISNSDGTTRPVGMIGK A STSDMLLKLARTTPYYKRNRRPHICSFVW*

human (170) KGECKRGECEPYRHEKPTDPPDDPLADQNIKDRYYGINDPVADKLLKRASTMPRLDPPEDKTIITLLYVGGLG---DTITETDLRNH
 mouse (170) KGECKRGECEPYRHEKPTDPPDDPLADQNIKDRYYGINDPVADKLLKRASTMPRLDPPEDKTIITLLYVGGLG---DTITETDLRNH
 zebrafish (170) KGECKRGECEPYRHEKPTDPPDDPLADQNIKDRYYGINDPVANKLLMRASTMPRLDVPDDKSIITLLYIGGLG---ENVHDSLELRNH
 drosophila (170) KGECKRGECEPYRHDKNEPDDPLCEQNIKDRYYGRNDPVAEKIMKRAASLPTLEPPEDRNITLLYVGNLP---EEITEPELRDQ
 C. Elegans (173) KGECKRGECEPYRHEKPTDPPDPLSRQNIKDRYYGTNDPVAEKILNRAAAAPTLSPPADTITLLYIGNLGPSSGAQQVTEKDLNDF
 Consensus (173) KGECKRGECEPYRHEKPTDPPDDPLADQNIKDRYYGINDPVADKLLKRASTMPRLDPPEDKTIITLLYVGGLG D ITETDLRNH*

human (252) FYQFGEIRTIIVVQRQQCAFIQFATRQAAEVAAEKSFNKLIVNGRRLNKWKGRSQAARGKEKEKDGTTDSGIKLEP---VPGLPGAL
 mouse (252) FYQFGEIRTIIVVQRQQCAFIQFATRQAAEVAAEKSFNKLIVNGRRLNKWKGRSQAARGKEKEKDGTTDSGIKLEP---VPGLPGAL
 zebrafish (252) FYQFGEIRTIIVVQRQQCAFIQFATRQAAETAAEKSFNKLIVNGRRLNKWKGRSQAARGKG-EKDGVTESGIRLEP---VPGLPGAL
 drosophila (252) FYQFGEIRSIALVPRQQCAFVQYTKRNSAELAAERTFNKLVIQGRKVSIKWAHSQAQKGTAAKTDRRRFDLAGIPPSAKPNDYFNL
 C. Elegans (259) FYQYGDIRCLRVLTEKGCFAFIEFTTREAAREAAERSFNKTFIKGKRLTIRWGEPOAKRAAD-----NSNYVTF--VPSVPIILP
 Consensus (259) FYQFGEIRTIIVVQRQQCAFIQFATRQAAEVAAEKSFNKLIVNGRRLNKWKGRSQAARGKE EKDG TDSGIKLEP VPGLPGAL

human (336) PPPPAAEEASANYFNLPSPGPPAVVNIALPPPPGIAAPPPPPGFGPHMFHPMG-----PPPPFMRAPGPIHYPSQDPQRMGAHAG
 mouse (336) PPPPAAEEASANYFNLPSPGPPAVVNIALPPPPGIAAPPPPPGFGPHMFHPMG-----PPPPFMRAPGPIHYPSQDPQRMGAHAG
 zebrafish (335) PPPPVSD EDASTNYFNLAFTPS PAVMNLGLPPPPGVMTMPPPGFGPPMFHTMDPMAVPPPPMALRPPGQVHYPSQDPQRMGAHAS
 drosophila (338) ROEQINVMPPAGMKLHQLPSNLVPASAYQMGQPTAAAYGNATSTALSSSGVN-LDSISIPPE---PGQVYPSQDASRMGAVKK
 C. Elegans (335) VPDGLAPSTSSQQRFITGSMRPPAPPTFAAPRSLVVPNVRFPVKAGESGASS-----SSIIYPSQDPTRLGAKGD
 Consensus (345) PPPPIAEEAS NYFNLPSPS PAVVNIALPPPPGIAAPPPPPGFGFP MFH M PPPP MR PG IHYPSQDPQRMGAHA

human (416) KHSSP
 mouse (416) KHSSP
 zebrafish (421) RHGGP
 drosophila (419) -----
 C. Elegans (406) VIE--
 Consensus (431) KH P

2.6. *In vitro* synthesis of zRBM22-EGFP mRNA, zALG2-mRFP-mRNA, EGFP-mRNA, mRFP-mRNA, and microinjection

The pSP64TNE-zRBM22-EGFP, pSP64TNE-zALG2-mRFP, pSP64TNE-EGFP and pSP64TNE-mRFP plasmids were linearized with XbaI. The zRBM22-EGFP-mRNA, zALG2-mRFP-mRNA, EGFP-mRNA, mRFP-mRNA were prepared and precipitated using the mMACHINE[®] sp6 Kit (Ambion) following the protocol recommended by the manufacturer.

Embryos were injected with ~ 300 pg to 400 pg mRNA into the yolk at the 1-cell stage. The microinjection pipettes and pressure injection system used were described previously [25]. Bright-field and fluorescence images of embryos at the 256-cell, 12-somite, and 20-somite stages, were captured with a Nikon C1 scanning confocal system using Nikon Fluor 20x/0.5NA and Nikon Fluor 40x/0.8NA water dipping objectives. EGFP fluorescence was captured using a 488 nm excitation filter and 515 to 530 (30-nm bandwidth) nm emission filter, while mRFP fluorescence was captured using a 543 nm excitation filter and 570 nm (long pass) emission filter. The co-localization analysis of the embryo that was co-injected with both zRBM22-EGFP-mRNA and the zALG2-mRFP-mRNA was determined using the “Measure Colocalization” function in Metamorph version 6.1 (Universal Imaging Corp., Downingtown, PA).

3. Results

ALG-2 was up-regulated in proliferating tissues [3,27]. To further understand the biology of ALG-2 we set to identify interacting targets of ALG-2. To date only a few partner proteins for ALG-2 were reported, namely AIP-1 [4] for ALG2 interacting protein 1 and Alix [5] for ALG2 interacting protein X which are identical proteins. The other targets included annexin VII, annexin XI [28] or HEED, the human embryonic ectoderm development protein [29]. The latter may be of special interest in the context described below. It was also reported that ALG-2 interacts with penta EF-Hand proteins like e.g. peflin to form heterodimers [30]. To search for new targets of ALG-2 we exploited a yeast two-hybrid screening on a human peripheral blood cDNA library using the full length cDNA of human ALG-2 as bait. After screening over 10⁶ clones 50 positive clones were identified that reacted positive after a second X-Gal filter test only in the presence of the ALG-2-plexA fusion bait using β -galactosidase as reporter. Fig. 2 shows a representative filter test in which the identified clones selected by the yeast

Table 1

ALG-2 targets selected by yeast two-hybrid screening with ALG-2 as bait

Clone	No.	Motif
Peflin	5	Penta EF-hand protein
ALG-2	3	Penta EF-hand protein
AIP-1	2	ALG-2 interacting protein
RBM22	2	RNA-binding protein containing a zinc finger of type C3H (Cx7Cx5Cx3H)
Annexin VII	2	Membrane protein
Annexin XI	2	Membrane protein

two-hybrid screening are indicated. Fig. 2 lane a shows a control using mock-transformed L40 yeast strains, lane b shows positive clones using L40 yeast strains in the presence of the fusion plasmid plexA-ALG-2. Table 1 lists the clones that were selected at least twice in the screen of those 25 library plasmids that were chosen for further analysis indicating that the screening procedure identified a number of targets of ALG-2 which were described also by others and are a good positive control of the screen.

In order to examine whether ALG-2 and RBM22 interacted with each other inside cells we prepared cDNA constructs encoding the two proteins fused to either enhanced green fluorescent protein (EGFP) to label RBM22 or monomeric red fluorescent protein (mRFP) to label ALG-2. Fusion between the fluorescent proteins and the proteins of interest have been arranged so that the fluorescent proteins were C-terminal to ALG-2 or RBM22, respectively i.e. the appearance of fluorescence within the cells indicated appropriate in frame expression of the fused proteins. Fig. 3A shows NIH 3T3 cells expressing the fusion protein ALG-2-mRFP whereas Fig. 3B displays a NIH 3T3 cell expressing RBM22-EGFP. Fig. 3A reveals a diffuse cytosolic localization of ALG-2-mRFP indicating that fusion of mRFP to ALG-2 does not lead to a translocation of the fused protein to the nucleus, an important prerequisite for functional studies of a cytosolic protein. On the other hand, RBM22 fused to EGFP was mainly found in the nucleus (Fig. 3B) as could be expected from an RNA-binding protein. However, if the two fusion proteins were co-expressed

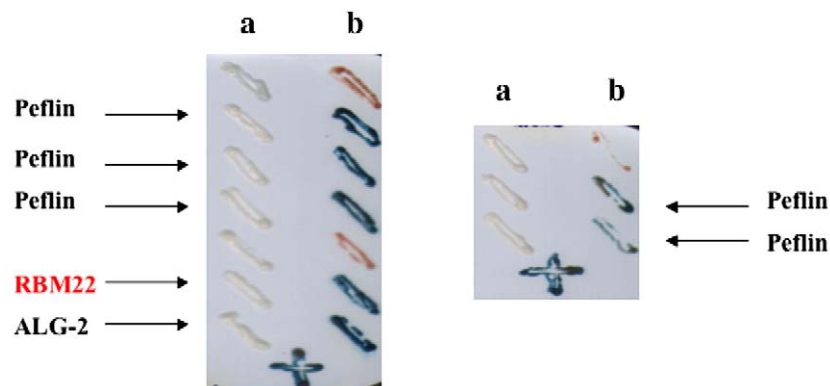


Fig. 2. Bait dependency test. Using ALG-2 as bait and human peripheral blood cDNA as library source more than 1 million yeast colonies were screened. Of the number of plasmids reacting positive after the second X-Gal filter test some were retransformed into yeast strain L40. **a**=transformation into L40+plexA; **b**=transformation into L40+plexA-ALG-2. The identified proteins are indicated. The blue crosses at the bottom of the 2 panels are positive controls for the development of the blue color of the β -galactosidase test.

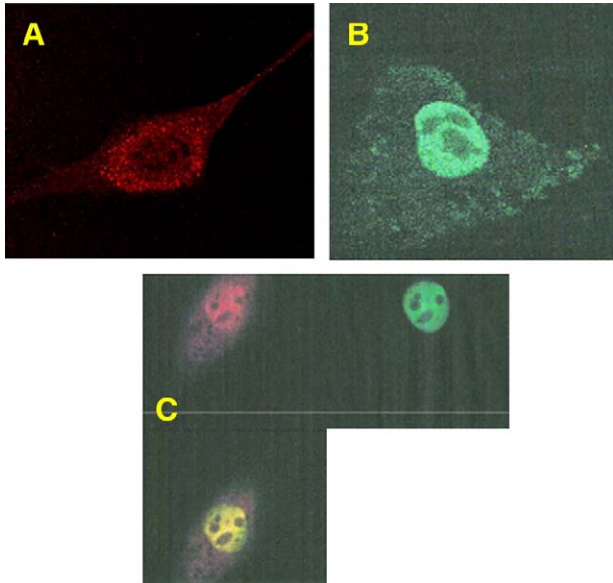


Fig. 3. Transfection of NIH 3T3 cells. The cells were transfected with expression vectors containing cDNA encoding either ALG2-mRFP (A), or RBM22-EGFP (B). In (C), NIH 3T3 cells were co-transfected with ALG2-mRFP and RBM22-EGFP and images were either taken with the filter for red fluorescence (left, excitation at 543 nm), green fluorescence (right, excitation at 488 nm) or merged (lower image).

in NIH 3T3 cells a major proportion of ALG2-mRFP could be found in the nucleus as indicated by merging the green and red fluorescent images which lead to a mainly yellow colored

nucleus (Fig. 3C). This result indicates that RBM22, which can shuttle between the cytosol and the nucleus using transportin-1 (J. Krebs, R. Falchetto, U. Kutay, unpublished results), interacts with ALG-2 intracellularly and assists in nuclear translocation of ALG-2.

The zebrafish (*Danio rerio*) is an excellent model organism to study physiological functions during development because of its transparency permitting the application of optical methods, especially fluorescence (see [31] for a recent review). Thus, RNAs encoding the fluorescent constructs of RBM22-EGFP and ALG2-mRFP using the zebrafish homologues of ALG-2 and RBM22, respectively, were microinjected into the yolk of 1-cell stage embryos, followed by confocal images capturing at various time intervals. Fluorescent signals from both fluorescent proteins could be observed as early as the 16-cell stage as can be seen from Fig. 4. However, the level of fluorescence produced by mRFP was much weaker than the corresponding signals of EGFP. Fig. 4 shows representative images captured at different time points after the 64-cell stage (2 h post fertilization; hpf) to the shield stage (6 hpf), both fluorescent proteins were evenly distributed throughout cells during development.

Fig. 5 shows images of a zebrafish embryo microinjected at the 1-cell stage with RNA of the ALG2-mRFP construct. The fluorescent signal was observed as early as the 16-cell stage (not shown), the earliest stage shown in Fig. 5 represents the 64-cell stage, and the images are shown up to the shield stage (6 hpf). ALG2-mRFP is distributed over whole cells, but some protein accumulated within the nucleus from 1K-cell stage

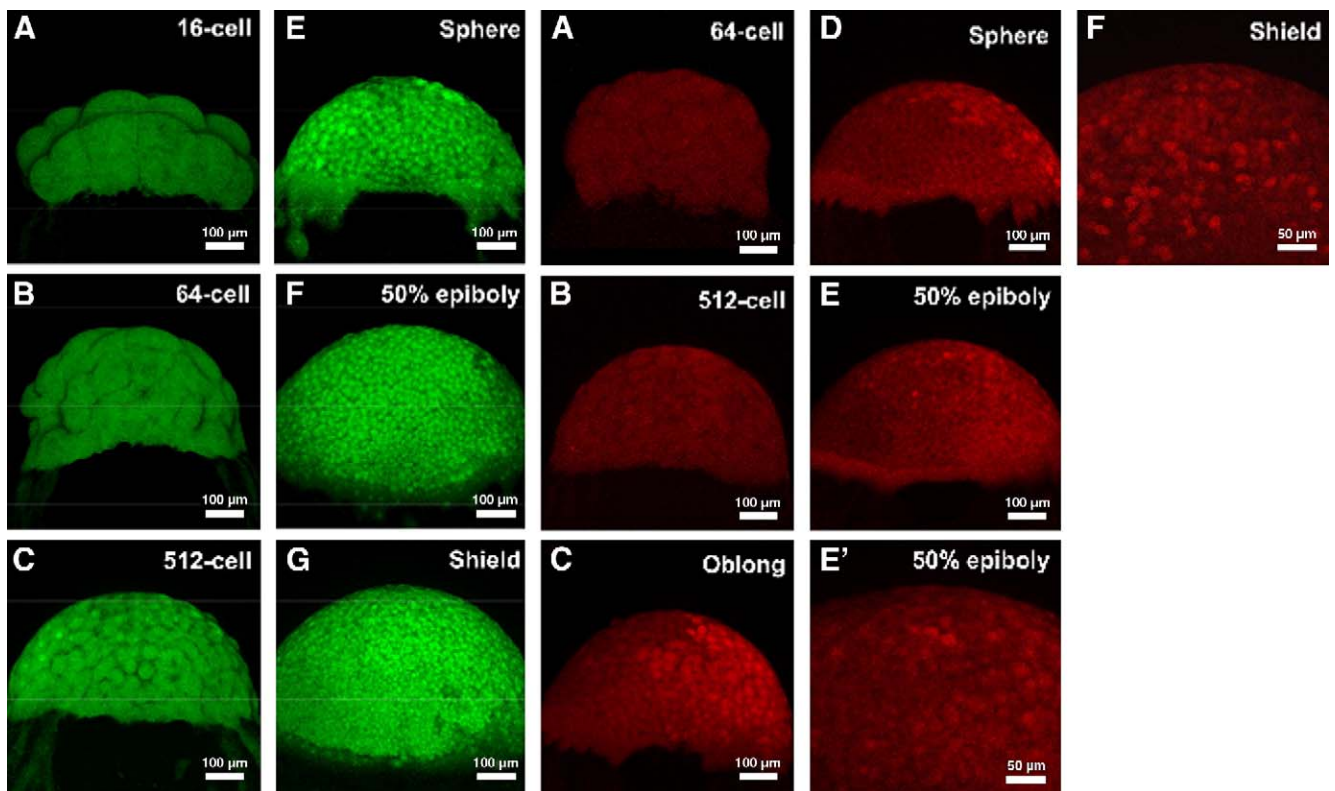


Fig. 4. Control images for EGFP and mRFP during zebrafish embryo development. The mRNAs of either EGFP (left series, A through G) or of mRFP (right series, A through F, E' is a 2-fold magnification of E) have been microinjected at the 1-cell stage of the embryo and confocal images have been captured at the different developmental stages as indicated.

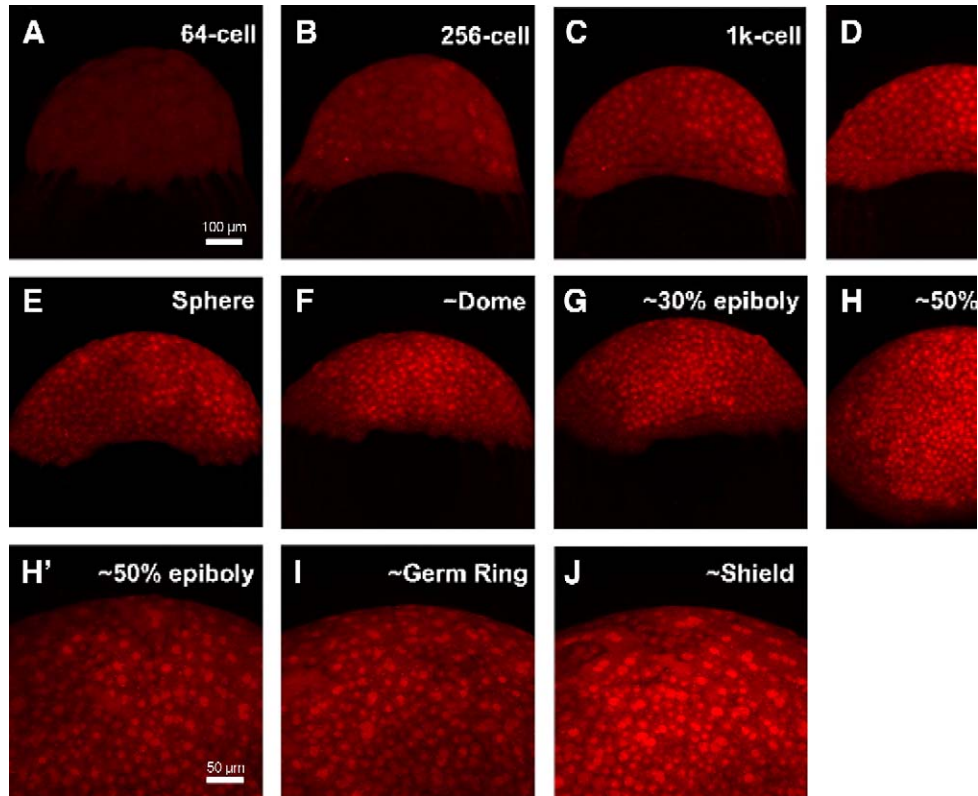


Fig. 5. Confocal images of ALG2-mRFP during zebrafish embryo development. mRNA of ALG2-mRFP has been microinjected at the 1-cell stage of the embryo and confocal images have been captured at the different stages of development as indicated (H' is a 2-fold magnification of H).

onwards, likely due to the presence of endogenous RBM22 (see below).

If the RNA encoding RBM22-EGFP was microinjected into zebrafish embryos at the 1-cell stage the fluorescent signals could be observed from the 16-cell stage embryo onwards like

in the controls (not shown). A representative fluorescent image of a 256-cell stage embryo (2.5 hpf) is shown in Fig. 6A indicating that at this stage RBM22-EGFP is distributed over the whole cell, but the protein starts to accumulate in the nucleus as documented as brighter spots within the nuclei. Nuclear

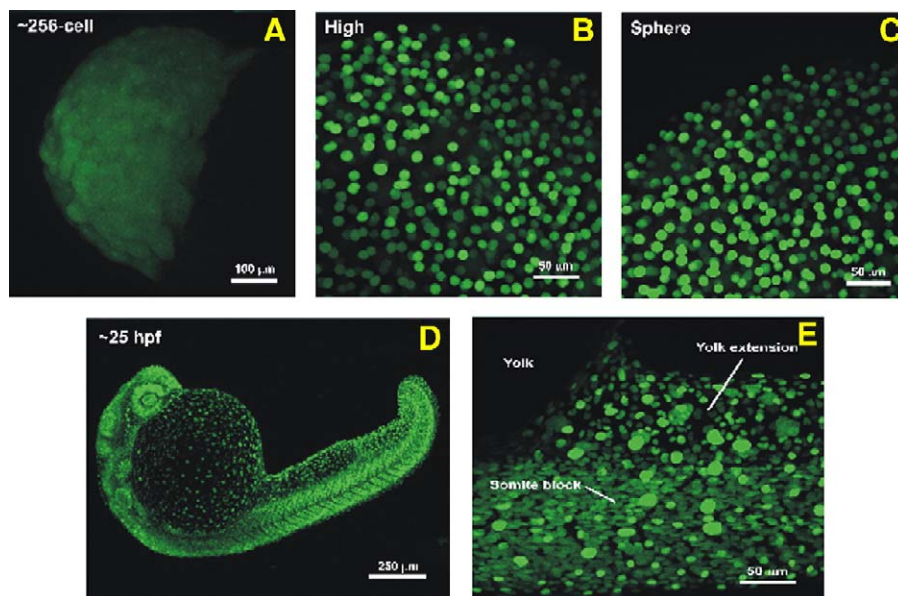


Fig. 6. Confocal images of RBM22-EGFP during zebrafish embryo development. mRNA of RBM22-EGFP has been microinjected at the 1-cell stage of the embryo and confocal images have been captured at the different stages of development as indicated. D shows even distribution of RBM22-EGFP over the whole body of the zebrafish embryo after 25 h of development, E is a 5-fold magnification of a somite area of 6D.

accumulation of RBM22 was evident at later stages (Fig. 6B and C) including embryos at high (3.3 hpf) and at sphere (4 hpf) stage, respectively, i.e. from high stage onwards RBM22 is exclusively localized within the nucleus. Fig. 6D provides evidence that RBM22-EGFP is distributed evenly over the whole body of the embryo (shown at prim-6, i.e. 25 hpf stage), Fig. 6E is a 5-fold magnification of a somite area in Fig. 6D.

Fig. 7 shows a time-dependent series of representative images of zebrafish embryos that have been co-injected with RNAs of ALG2-mRFP and RBM22-EGFP at the 1-cell stage.

At the 64-cell stage ALG2-mRFP was hardly observable (Fig. 7A), therefore merging the green fluorescence from RBM22-EGFP with the red fluorescence from ALG2-mRFP resulted in a green image at the bottom. However, as seen at the next stage, i.e. 256-cell stage (Fig. 7B), ALG2-mRFP started to accumulate in the nucleus indicating that the presence of RBM22 helps to translocate ALG-2 into the nucleus as evidenced by the merging of the two confocal images resulting in yellow colored nuclei at the bottom of Fig. 7B. This observation was made through all stages of the embryo development up to stage “shield” as shown in Fig. 7J. By comparing the brightness of the yellow spots at

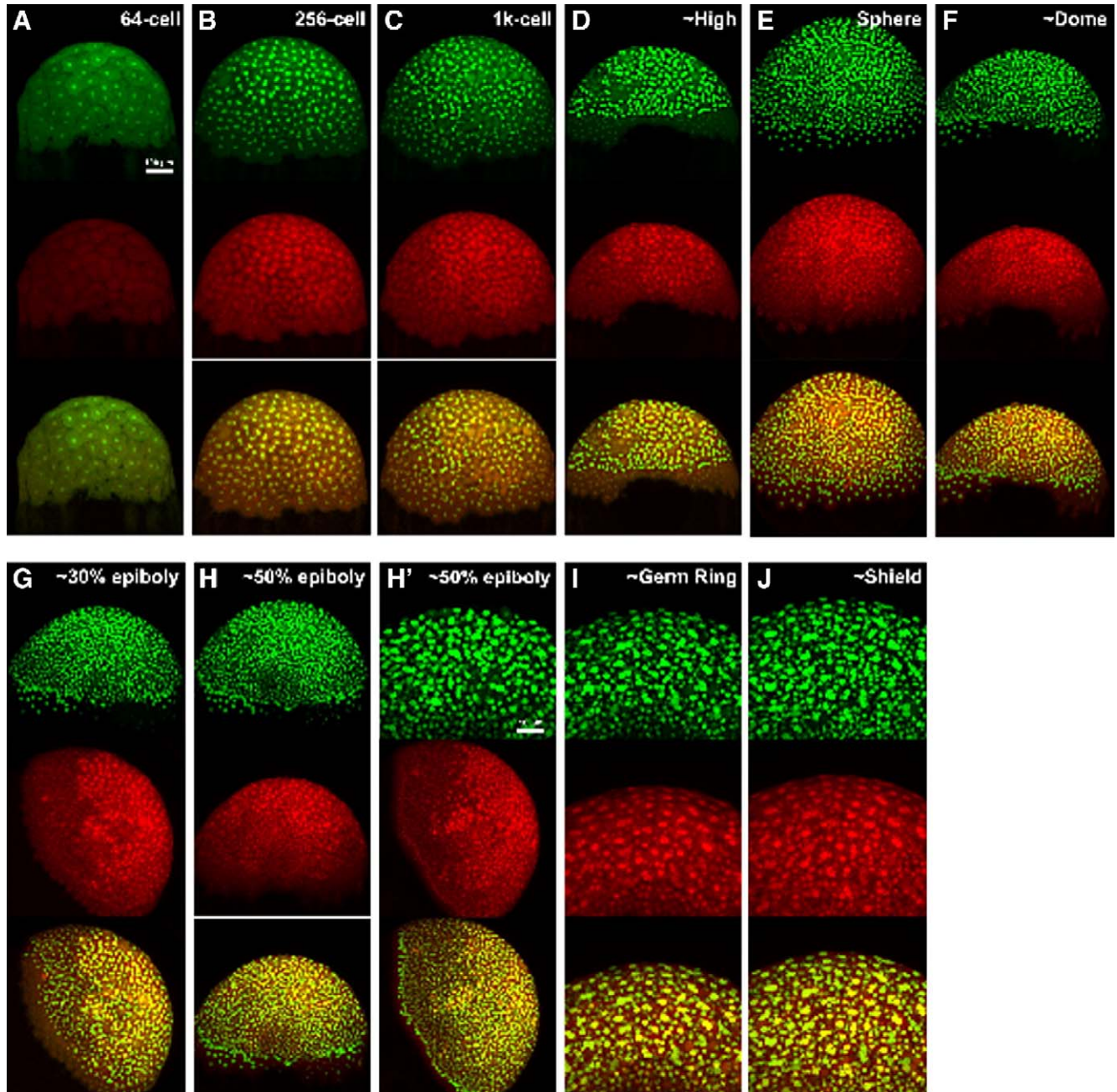


Fig. 7. Confocal images of co-injected ALG2-mRFP and RBM22-EGFP during zebrafish embryo development. mRNAs of ALG2-mRFP and RBM22-EGFP have been co-injected at the 1-cell stage of the embryo and confocal images have been captured at the different developmental stages as indicated. The upper rows of images (green fluorescence) represents RBM22-EGFP, the middle row (red fluorescence) ALG2-mRFP and the lower row (yellow images) the merge of the upper 2 image rows indicating the co-localization of the 2 proteins within the nucleus during zebrafish development.

the bottom of the different pictures, i.e. Fig. 7B–J, the intensity of the fluorescence increased indicating the efficiency of the translocation of ALG-2 into the nucleus. Quantitation demonstrated that – depending on the available resolution – more than 95% of the 2 proteins co-localized within the same area of the nucleus indicating that they form a functional complex within the nucleus.

4. Discussion

In the present paper we demonstrate that the cytosolic protein ALG-2 (Fig. 3A) translocates to the nucleus (Figs. 3C and 7) in the presence of RBM22. This is shown by laser-scanning confocal microscopy of NIH 3T3 cells (Fig. 3) or zebrafish embryos during development (Fig. 7) expressing fluorescence tagged ALG-2 and RBM22 either alone or together. Over-expression of the 2 fluorescent constructs did not influence the normal development of the zebrafish embryos. The translocation of ALG-2 into the nucleus could already be observed in images of zebrafish embryos even if only ALG2-mRFP was microinjected at the 1-cell stage (Fig. 5) indicating that the endogenous presence of RBM22 was sufficient to assist in translocating ALG-2 into the nucleus. This translocation was not induced by the presence of the fluorescent proteins since control experiments with the fluorescent proteins alone did not provide any evidence for the accumulation of either protein within the nucleus (Fig. 4). Nuclear translocation of ALG-2 was earlier reported by Kitaura et al. [30] who detected ALG-2 in the nuclei of Jurkat T-cells. This translocation of ALG-2 into the nuclei of T-cells could be due to the interaction with RBM22 which is especially enriched in T-cells (J. Krebs, unpublished observations).

It remains to be shown how the two proteins interact. In a recent publication by Shibata et al. [32] the authors identified a region in the amino acid sequence of Alix/AIP1 responsible for the interaction with ALG-2. This part is rich in prolines and contains four tandem-repeats of PxY that are crucial for the interaction with ALG-2 as shown by replacement with alanines. The C-terminal part of RBM22 is rich in prolines (including several tetraproline sequences) and glycines, and the N-terminal region contains several PY or PF pairs, but how RBM22 interacts with ALG-2 has to await further experiments.

As shown in Fig. 1 RBM22 is a highly conserved RNA-binding protein, the human and mouse proteins being identical. Comparing the mammalian sequence with those of zebrafish, *Drosophila* or *C. elegans* the homologies between these proteins are 75% or better. If one compares the domain structures, i.e. the RNA-binding domains or the unusual zinc finger of the type Cx8Cx5Cx3H, the homologies are even higher. On the other hand, in the yeast homologue slt11 [6,33] or ECM2 [7] only the RNA-binding domain is conserved, but the zinc finger types are different. These proteins have been identified as splicing factors [6,33]. Rappsilber et al. [17] and Makarova et al. [34] identified the mammalian homolog of ECM2 (which is identical with RBM22) as a member of the mammalian spliceosome.

In a genome wide screening Graveley and co-workers identified regulators of alternative splicing by RNA interference in *Drosophila* [20]. One of the identified regulators, cg14641, is the *Drosophila* homolog of RBM22 responsible – among others – for the regulation of exon 4 splicing of the Dscam gene of *Drosophila* [20]. Alternative splicing, in general, is regulated by proteins associating with the pre-mRNA, and function either to enhance or to suppress the ability of the spliceosome to recognize the splice site(s) flanking the regulated exon. Kim et al. [23] while studying genes essential for heart development in *Drosophila* reported that cg14641 is one of those essential genes. In another study Kittler et al. [21] identified genes essential for cell cycle progression by an RNA interference screening of HeLa cells. Among the described 37 genes required for cell division the RBM22 homologue was identified next to other splicing factors known to generate mitotic spindle defects if knocked down. Finally, Hopkins' group reported that in a genome wide insertional mutagenesis screening of early zebrafish development 315 genes could be identified as being essential during this period, all being highly conserved during evolution [22]. One of the identified genes is the zebrafish homologue of RBM22. In all these investigations described before it became evident that RBM22 may be involved in developmental processes in which the regulation of alternative splicing of cytoskeletal proteins could become important like in *Drosophila* for the Dscam gene which is essential for neuronal outgrowth and target recognition [35]. Interestingly, another target interacting with ALG-2, HEED [29], is a transcriptional repressor involved in the regulation of homeotic genes during mouse development [36]. In the future it will be important to show how Ca²⁺-signaling could become involved in the regulation of alternative splicing due to the interaction between RBM22 and the Ca²⁺-binding protein ALG-2.

In conclusion, in the present paper we provided evidence for the functional interaction between the Ca²⁺-binding protein ALG-2 and the RNA-binding protein RBM22 in tissue cultures as well as in zebrafish embryonal development. This may provide a previously not described link between Ca²⁺-controlled signaling and the regulation of alternative splicing influencing basic cellular processes during development.

Acknowledgments

We would like to express our gratitude to Dr. Roger Y. Tsien, University of California, San Diego, USA, for providing us with the cDNA of monomeric red fluorescent protein (mRFP). We thank DUAL Systems Biotech AG, Zurich, Switzerland, for the excellent performance of the yeast two hybrid screening. Special thanks to Prof. Christian Griesinger, Head of the NMR based Structural Biology Department at the Max Planck Institute for Biophysical Chemistry, Göttingen, Germany, for his continuous support. Marek Michalak is a CIHR Senior Investigator, supported by CIHR. Work carried out in the laboratory of Andrew L. Miller was funded by the Hong Kong Research Grants Council awards HKUST 6279/03M and HKUST 6241/04M, and carried out when Dr. Miller was a

recipient of a Croucher Senior Research Fellowship. The present work was supported by the Max Planck Society.

References

- [1] E. Carafoli, Calcium signaling: a tale for all seasons, *Proc. Natl. Acad. Sci. U. S. A.* 99 (2002) 1115–1122.
- [2] J. Krebs, R. Klemenz, The ALG-2/AIP-complex, a modulator at the interface between cell proliferation and cell death? Hypothesis *Biochim. Biophys. Acta* 1498 (2000) 153–161.
- [3] J. Krebs, P. Saremaslani, R. Caduff, ALG-2: A Ca²⁺-binding modulator protein involved in cell proliferation and cell death, *Biochim. Biophys. Acta* 1600 (2002) 68–73.
- [4] P. Vito, L. Pellegrini, C. Quiet, Cloning of AIP1, a novel protein that associates with the apoptosis-linked gene ALG-2 in a Ca²⁺-dependent reaction, *J. Biol. Chem.* 274 (1999) 1533–1540.
- [5] M. Missotten, A. Nichols, K. Rieger, R. Sadoul, A novel mouse protein undergoing calcium-dependent with the apoptosis-linked-gene 2 (ALG-2) protein, *Cell Death Differ.* 6 (1999) 124–129.
- [6] D. Xu, J.D. Friesen, Splicing factor slt1p and its involvement in formation of U2/U6 helix II in activation of the yeast spliceosome, *Mol. Cell. Biol.* 21 (2001) 1011–1023.
- [7] M. Lussier, A.M. White, J. Sheraton, T. Di Paolo, J. Treadwell, S.B. Southard, C.I. Horenstein, J. Chen-Weiner, A.F.J. Ram, J.C. Kapteyn, T.W. Roemer, D.H. Vo, D.C. Bondoc, J. Hall, W.W. Zhong, A.M. Sdicu, J. Davies, F.M. Klis, P.W. Robbins, H. Bussey, Large scale identification of genes involved in cell surface biosynthesis and architecture of *Saccharomyces cerevisiae*, *Genetics* 147 (1997) 435–450.
- [8] S.F. Altschul, W. Gish, W. Miller, E.W. Myers, D.J. Lipman, Basic local alignment search tool, *J. Mol. Biol.* 215 (1990) 403–410.
- [9] S.F. Altschul, T.L. Madden, A.A. Schäffer, J. Zhang, Z. Zhang, W. Miller, D.J. Lipman, Gapped BLAST and PSI-BLAST: a new generation of protein database search programs, *Nucleic Acids Res.* 25 (1997) 3389–3402.
- [10] E.S. Lander, et al., Initial sequencing and analysis of the human genome, *Nature* 409 (2001) 860–921.
- [11] J.C. Venter, et al., The sequence of the human genome, *Science* 291 (2001) 1304–1351.
- [12] B.R. Graveley, Alternative splicing: increasing diversity in the proteomic world, *Trends Genet.* 17 (2001) 100–107.
- [13] D.L. Black, Alternative pre-mRNA splicing and neuronal function, *Annu. Rev. Biochem.* 72 (2003) 291–336.
- [14] B. Modrek, C.J. Lee, Alternative splicing in the human, mouse and rat genomes is associated with an increased frequency of exon creation and/or loss, *Nat. Genet.* 34 (2003) 177–180.
- [15] J.M. Johnson, J. Castle, P. Garnett-Engle, Z. Kan, P.M. Loerch, R. Armour, R. Santos, E.E. Schadt, R. Stoughton, D.D. Shoemaker, Genome-wide survey of human alternative pre-mRNA splicing with exon junction microarrays, *Science* 302 (2003) 2141–2144.
- [16] K. Hartmuth, H. Urlaub, H.P. Vornlocher, C.L. Will, M. Gentzel, M. Wilm, R. Luhrmann, Protein composition of human prespliceosomes isolated by a tobramycin affinity-selection method, *Proc. Natl. Acad. Sci. U. S. A.* 99 (2002) 16719–16724.
- [17] J. Rappsilber, U. Ryder, A.I. Lamond, M. Mann, Large-scale proteomic analysis of the human spliceosome, *Genome Res.* 12 (2002) 1231–1245.
- [18] M. Azubel, S.G. Wolf, J. Sperling, R. Sperling, Three-dimensional structure of the native spliceosome by cryo-electron microscopy, *Mol. Cell* 15 (2004) 833–839.
- [19] J.P. Venables, Aberrant and alternative splicing in cancer, *Cancer Res.* 64 (2004) 7647–7654.
- [20] J.W. Park, K. Parisky, A.M. Celotto, R.A. Reenan, B.R. Graveley, Identification of alternative splicing regulators by RNA interference in *Drosophila*, *Proc. Natl. Acad. Sci. U. S. A.* 101 (2004) 15974–15979.
- [21] R. Kittler, G. Putz, L. Pelletier, I. Poser, A.K. Heninger, D. Drechsel, S. Fischer, I. Konstantinova, B. Habermann, H. Grabner, M.L. Yaspo, H. Himmelbauer, B. Korn, K. Neugebauer, M.T. Pisabarro, F. Buchholz, An endoribonuclease –prepared siRNA screen in human cells identifies genes essential for cell division, *Nature* 432 (2004) 1036–1040.
- [22] A. Amsterdam, R.M. Nissen, Z. Sun, E.C. Swindell, S. Farrington, N. Hopkins, Identification of 315 genes essential for early zebrafish development, *Proc. Natl. Acad. Sci. U. S. A.* 101 (2004) 12792–12797.
- [23] Y.O. Kim, S.J. Park, R.S. Balaban, M. Nirenberg, Y. Kim, A functional genomic screen for cardiogenic genes using RNA interference in developing *Drosophila* embryos, *Proc. Natl. Acad. Sci. U. S. A.* 101 (2004) 159–164.
- [24] M. Westerfield, *The Zebrafish Book: A Guide for the Laboratory Use of Zebrafish (Brachidanio rerio)*, Univ. of Oregon Press, Eugene, OR, 1994.
- [25] S.E. Webb, K.W. Lee, E. Karplus, A.L. Miller, Localized calcium transients accompany furrow positioning, propagation, and deepening during the early cleavage period of zebrafish embryos, *Dev. Biol.* 192 (1997) 78–92.
- [26] P.A. Krieg, D.A. Melton, Functional messenger RNAs are produced by SP6 *in vitro* transcription of cloned cDNAs, *Nucleic Acid Res.* 12 (1984) 7057–7070.
- [27] J.M. La Cour, J. Mollerup, P. Winding, S. Tarabykina, M. Sehested, M.W. Berchtold, Upregulation of ALG-2 in hepatomas and lung cancer tissue, *Am. J. Pathol.* 163 (2003) 81–89.
- [28] H. Satoh, Y. Nakano, H. Shibata, M. Maki, The penta-EF-hand domain of ALG-2 interacts with amino terminal domains of both annexin VII and annexin XI in a Ca²⁺-dependent manner, *Biochim. Biophys. Acta* 1600 (2002) 61–67.
- [29] K.H. Lee, E. Kim, J.S. Lee, K.S. Lee, J.W. Kim, Mapping of the interaction sites between apoptosis linked gene ALG-2 and HEED, *Mol. Cells* 12 (2001) 298–303.
- [30] Y. Kitaura, S. Matsumoto, H. Satoh, K. Hitorni, M. Maki, Peflin and ALG-2, members of the penta-EF-Hand protein family, form a heterodimer that dissociates in a Ca²⁺-dependent manner, *J. Biol. Chem.* 276 (2001) 14053–14058.
- [31] S.E. Webb, A.L. Miller, Calcium signalling during zebrafish embryonic development, *BioEssays* 22 (2000) 113–123.
- [32] H. Shibata, K. Yamada, T. Mizuno, C. Yorikawa, H. Takahashi, H. Satoh, Y. Kitaura, M. Maki, The penta-EF-hand protein ALG-2 interacts with a region containing PxY repeats in Alix/AIP1, which is required for the subcellular punctate distribution of the amino-terminal truncation form of Alix/AIP1, *J. Biochem. (Tokyo)* 135 (2004) 117–128.
- [33] D. Xu, D.J. Field, S.J. Tang, A. Moris, B.P. Bobechko, J.D. Friesen, Synthetic lethality of yeast slt mutations with U2 small nuclear RNA mutations suggest functional interactions between U2 and U5 snRNPs that are important for both steps of pre-mRNA splicing, *Mol. Cell. Biol.* 18 (1998) 2055–2066.
- [34] O.V. Makarova, E.M. Makarov, H. Urlaub, C.L. Will, M. Gentzel, M. Wilm, R. Luhrmann, A subset of human 35S U5 proteins, including Prp19, function prior to catalytic step 1 of splicing, *EMBO J.* 23 (2004) 2381–2391.
- [35] B.E. Chen, M. Kondo, A. Garnier, F.L. Watson, R. Puettmann-holgado, D. R. Lamar, D. Schmucker, The molecular diversity of Dscam is functionally required for neuronal wiring specificity in *Drosophila*, *Cell* 125 (2006) 607–620.
- [36] O.N. Denisenko, K. Bomsztyk, The product of the murine homolog of the *Drosophila* extra sex combs gene displays transcriptional repressor activity, *Mol. Cell. Biol.* 17 (1997) 4707–4717.